**Other materials** were commercially available compounds and purified prior to use, if necessary, by destillation or sublimation.

**Acknowledgment.** This work was supported by the Deutsche Forschungsgemeinschaft, by the Fonds der Chemischen Industrie, and by the Universität des Saarlandes.

**Supplementary Material Available.** A listing of $^{13}C$ shifts for all measured compounds at various temperatures (3 pages). Ordering information is given on any current masthead page.

## References and Notes

(1) Part X of "$^{13}$CMR Spectroscopical and Stereochemical Investigations"; part IX: H.-J. Schneider and E. F. Weigand, *Tetrahedron*, **31**, 2125 (1975).
(2) J. W. Emsley, J. Feeney, and L. M. Sutcliffe, "High Resolution Nuclear Magnetic Resonance Spectroscopy", Vol. 1, Pergamon Press, London, 1965, pp 99–103.
(3) See (a) J. Ando and A. Nishioka, *Bull. Chem. Soc. Jpn.*, **46**, 706 (1973); (b) W. M. Litchman and D. R. McLaughlin, *Chem. Phys. Lett.*, **22**, 424 (1973). The differential temperature dependences for hydrocarbons reported in this work were not recognized in these papers[3b] and were assumed to be larger for $\delta_{CH_2}$ than for $\delta_{CH_3}$ in *n*-butane.[3a]
(4) H.-J. Schneider, M. Schommer, and W. Freitag, *J. Magn. Reson.*, **18**, 393 (1975).
(5) A. K. Jameson and C. J. Jameson, *J. Am. Chem. Soc.*, **95**, 8559 (1973).
(6) Chemical shift values are available as supplementary material. See the paragraph at end of paper.
(7) Compare R. M. Stevens and M. Karplus, *J. Chem. Phys.*, **49**, 1094 (1968); W. T. Raynes and G. Stanney, *J. Magn. Reson.*, **14**, 378 (1974).
(8) M. Karplus and J. A. Pople, *J. Chem. Phys.*, **38**, 2803 (1963); M. Karplus and T. B. Das, *ibid.*, **34**, 1683 (1961); J. A. Pople *ibid.*, **37**, 53, 60 (1962).
(9) A. D. Buckingham, *Can. J. Chem.*, **38**, 300 (1960).
(10) J. Feeney, L. H. Sutcliffe, and S. M. Walker, *Mol. Phys.*, **11**, 117, 137 (1966).
(11) R. J. W. LeFèvre, *Aust. J. Chem.*, **14**, 312 (1961).
(12) R. S. Armstrong, M. Aroney, C. G. LeFèvre, R. J. W. LeFèvre, and M. R. Smith, *J. Chem. Soc.*, 1474 (1958).
(13) H.-J. Schneider and W. Freitag, unpublished results.
(14) For a recent discussion of reaction fields, see E. Grunwald, S. Highsmith, and Ting-Pol in "Ions and Ion Pairs in Organic Reactions", Vol. 2, M. Szwarc, Ed., Wiley, New York, N.Y., 1974, p 449.
(15) M. Landolt and R. Börnstein, "Zahlenwerte und Funktionen", Vol. II /6, Springer-Verlag, Berlin, 1950, p 669.
(16) D. K. Dalling and D. M. Grant, *J. Am. Chem. Soc.*, **89**, 6612 (1967); *ibid.*, **94**, 5318 (1972); H.-J. Schneider, R. Price, and T. Keller, *Angew. Chem.*, **83**, 759 (1971); *Angew. Chem., Int. Ed. Engl.*, **10**, 730 (1971).
(17) $^{13}$CMR shifts in cholestane show temperature dependences similar to those described in this paper: H.-J. Schneider and W. Gschwendtner, unpublished results.
(18) This method has been used with temperature dependent coupling constants: H. S. Gutowsky, G. G. Belford, and P. E. McMahon, *J. Chem. Phys.*, **36**, 3353 (1962); G. Govil and H. J. Bernstein, *ibid.*, **47**, 2818 (1967).
(19) P. B. Wolter and E. W. Garbisch, Jr., *J. Am. Chem. Soc.*, **94**, 5310 (1972).

# Resonance Raman Study of the Thermochromic Phase Transition of a Polydiacetylene

**Gregory J. Exarhos,[1a] William M. Risen, Jr.,*[1a] and Ray H. Baughman[1b]**

*Contribution from the Department of Chemistry, Brown University, Providence, Rhode Island 02912, and the Materials Research Center, Allied Chemical Corporation, Morristown, New Jersey 07960.* *Received April 7, 1975*

**Abstract:** Polymers of the type $[=C(R)—C\equiv C—(R)C=]_n$, obtained by the solid-state polymerization of the corresponding diacetylene, have substantial $\pi$-electron delocalization along the chain, forming a pseudo-one-dimensional electronic system. The polymer poly-ETCD, of this form, where R is $-(CH_2)_4OCONHC_2H_5$, has a nearly reversible (green-red) thermochromic phase transition in the 117–137°C range. Its Raman spectra reveal dramatic changes in the frequency and intensity of $\nu(C=C)$ and $\nu(C\equiv C)$ bands as a function of source frequency and of temperature, as it is raised through the transition. The changes result from the thermal transition and from selective resonance enhancement of vibrations for domains with whose electronic transitions the source is in resonance. The $\pi$-electron delocalization is thus shown by resonance Raman spectroscopy to occur over segments, or domains, along the polymer backbone. The distribution of the "delocalization lengths" is peaked at three values at 25°C but at one value above the transition, for poly-ETCD samples prepared by 100 Mrad $\gamma$-ray irradiation. Energy level calculations are consistent with a delocalization-length distribution peaked around 3.0–8.0 nm, and above 20.0 nm at 25°C and at about 8.0 nm above the transition.

Crystalline materials formed by the solid-state polymerization of diacetylene monomers, of the form $RC\equiv CC\equiv CR$, are under investigation because $\pi$-electron density can be delocalized extensively along the polymeric chains.[2-7] This extended, conjugated, $\pi$-bond structure can be described by two resonance forms:

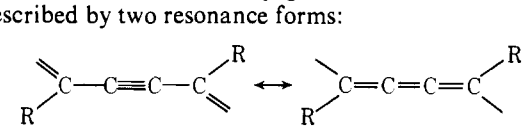

Intense $\nu(C=C)$ and $\nu(C\equiv C)$ vibrational bands observed in the Raman spectra indicate that the acetylenic structure predominates, but the relatively low frequencies of these vibrations and the linear correlation between them show that there is a substantial "resonance admixture" of the butatriene structure.[2,3]

Electron delocalization can be over a distance as long as the chain length of a polymer molecule, but it can be over shorter distances if continuity of "conjugation" is broken by configurational or chemical (functional group) defects. The chain lengths of the molecules are limited only by breaks which represent crystal defects. These defects are responsible for a distribution of chain lengths. There can be a distribution of configurations of the individual polymer molecules as well, so overall we may expect that in general there will be many "delocalization lengths" over which $\pi$-electron delocalization is uninterrupted.

Since the extent of $\pi$-electron delocalization along the backbone of the linear polymer chains should affect the optical properties of these materials strongly, optical absorbance and Raman scattering experiments should yield information about the distribution of $\pi$-electron delocalization lengths in a polydiacetylene.

In earlier Raman spectral studies of polydiacetylenes[2] it was found that the strong Raman bands appear in the $\nu(C=C)$ and $\nu(C\equiv C)$ regions and are at relatively low

frequencies. The value of $\nu$(C=C) was found to vary linearly with $\nu$(C≡C) as the R groups and/or phase perfections were changed in a series of such polymers.[3] These results were interpreted as an indication that $\pi$-electron delocalization is important in understanding the optical properties of polydiacetylenes.

When the R groups in a diacetylene are $(CH_2)_4O$-$CONHC_2H_5$ the resultant polymerized material is known trivially as poly-ETCD, and will be referred to as that hereinafter. Poly-ETCD appears to be green in reflection at room temperature, but at about 135°C it undergoes a nearly reversible green-to-red phase transition.

In this paper we report our study of the thermochromic phase transition of poly-ETCD by measurement and analyses of the temperature-dependent resonance Raman spectral changes associated with the color change. The analysis of the resonance Raman and optical absorption results together are shown to probe the distribution of $\pi$-electron delocalization lengths in the polymer, represented by:

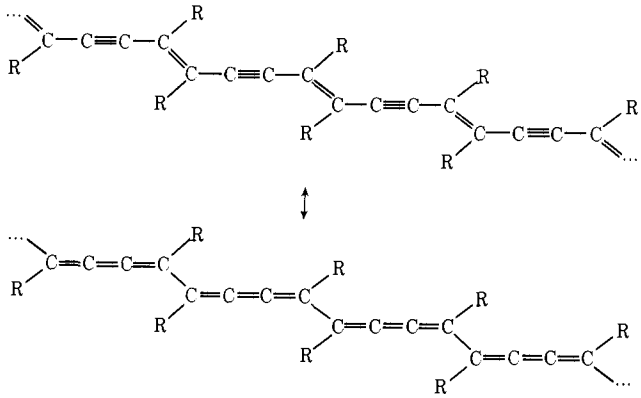

## Experimental Section

Poly-ETCD was prepared by irradiating single crystals of the diacetylene monomer, $RC_4R$, where R is $(CH_2)_4OCONHC_2H_5$, with $^{60}Co$ $\gamma$ rays at dosage rates for various samples of 1, 5, 25, 50, or 100 Mrad. Residual monomeric material was extracted from the polymer with methanol. The samples irradiated at 25, 50, or 100 Mrad appear green (in reflection) at room temperature but "reversibly" become red at about 135°C. The lower dosage samples are red at all temperatures below the melting point, which is above 200°C. These spectral studies were carried out on 100 Mrad samples.

The visible absorption spectrum of poly-ETCD was measured on a finely powdered sample dispersed in KBr with a Cary 14 spectrometer.

Raman spectra of poly-ETCD were measured with 90° scattering geometry on a Jarrell-Ash 25-300 Raman spectrometer using the principal lines of Kr and Ar ion lasers at low power as sources. For the room-temperature Raman measurements, the polymer was sandwiched between two thin glass plates and this sample unit was mounted on a rotating sample device. During measurements the sample was spun at 1000 rpm to minimize any possible decomposition resulting from the absorption of the visible light of the source. Raman spectra measured at higher temperatures also were obtained with 90° scattering from the polymer sandwiched between glass plates. In this case, however, the sample unit was mounted, with good thermal contact, on a metal block whose support shaft was wound with resistive heating wire. This assembly was supported in a glass cylinder containing several pounds of lead shot, such that only the block and sample protruded, and a cover plate was placed over the cylinder. Using this setup, temperature was controlled proportionately to within 0.5°C, as measured by a sensor on the sample block, and no optical distortions were observed. Spectra at temperatures in the 25-200°C range were measured in this fashion with sources of 1 mW at 632.8 nm, and 10 mW at each principal line of the Ar and Kr ion lasers.

Thermogravimetric analyses (TGA) and differential thermal analysis (DTA) were performed on 5-mg samples of poly-ETCD in the 25-500°C range at a heating rate of 10°C per min. Differential scanning calorimetry (DSC) was utilized on 5-mg samples to measure the phase transition. In this case the heating rate was 5°C per min in the 25-150°C range.

## Results

**Absorption Spectra.** The visible absorption spectrum of poly-ETCD, shown in Figure 1, has three very broad structureless features which appear to be due to the overlap of three bands, all of which are superimposed in Figure 1 on the low-frequency wing, decreasing as the frequency decreases, due largely to the KBr matrix in the region shown. The three occur at 460, 540, and 630 nm. Since the R group in this material is not a chromophore in the visible region, the absorptions which give rise to these three bands are assigned to transitions in $\pi$-electron systems along the polymer backbone. A *simple* model for the electronic structure of such a system is that of a one-dimensional free electron gas, or particle-in-a-box. Although the use of this model will be discussed in a later section, the concept can be employed to assign the bands to the first allowed transition of such an electron gas to an excited state, in boxes of three different lengths. Such an interpretation implies that although there is a continuous distribution of the many different lengths of polymer over which $\pi$-electrons are delocalized, at room temperature the distribution of these lengths is peaked around three lengths.

**Room-Temperature Raman Spectra.** The Raman spectra of poly-ETCD taken with various light sources are different, although in each the two strongest features are due to the carbon-carbon double bond stretch, $\nu$(C=C), and the carbon-carbon triple bond stretch, $\nu$(C≡C), along the polymer chain.

When the spectrum is excited by red light, either He-Ne 632.8 nm or Kr 647.1 nm, the spectrum shown in Figure 2 (top) is observed. Here $\nu$(C≡C) is found at 2078 $cm^{-1}$, $\nu$(C=C) is at 1454 $cm^{-1}$, and a strong feature is observed at 1254 $cm^{-1}$, which may be due to a $\nu$(C-C) mode. The vibrations of the R groups, which dominate the infrared spectrum of poly-ETCD, are weak or absent, as are those from chain-bending vibrations.

As shown in Figure 2 (bottom), when the Raman spectrum is excited by yellow light, Kr 568.2 nm, the strong bands are changed in position and intensity from what they are when the spectrum is excited by red light. In particular, the $\nu$(C≡C) band is found 26 $cm^{-1}$ higher, at 2104 $cm^{-1}$, and the $\nu$(C=C) band is found 42 $cm^{-1}$ higher, at 1496 $cm^{-1}$. The 1254-$cm^{-1}$ band has been replaced by weak bands in the 1150-1250-$cm^{-1}$ region.

This variation of $\nu$(C=C) and $\nu$(C≡C) with source frequency results in the observation of a third $\nu$(C=C) value, 1525 $cm^{-1}$, at which a band appears when green, 514.5 nm Ar, or blue, 488.0 nm Ar, radiation is used. This is shown in Figure 3. An analogous effect on $\nu$(C≡C) is observed.

The positions of the 632.8-, 530.8-, and 457.9-nm source lines are marked on Figure 1 to show their proximity to the absorbance bands of poly-ETCD. Each is so located as to come into resonance with the electronic transition of a polymer segment of a given $\pi$-electron delocalization length. This and the appearance of three vibrational frequencies for $\nu$(C=C) and $\nu$(C≡C) are interpreted as follows.

The lengths of $\pi$-electron delocalization (delocalization lengths) which occur at room temperature in poly-ETCD are distributed around three values, which we may call $l_1$, $l_2$, and $l_3$, and we call the polymer segments of these lengths domains 1, 2, and 3. If light of the proper wavelength to cause the $\pi$-electron transition in domain 1 is used as the Raman source, the vibrations proper to that domain will give rise to the greatest Raman scattering via the resonance

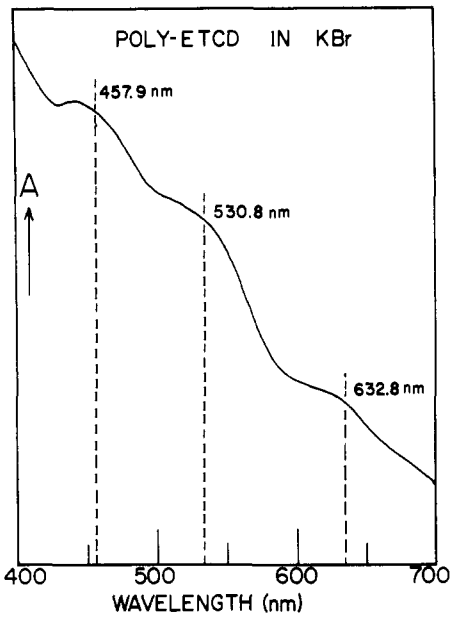


Figure 1. Visible absorption spectrum of solid poly-ETCD dispersed in KBr. There is no compensation for the KBr matrix made on this spectrum.

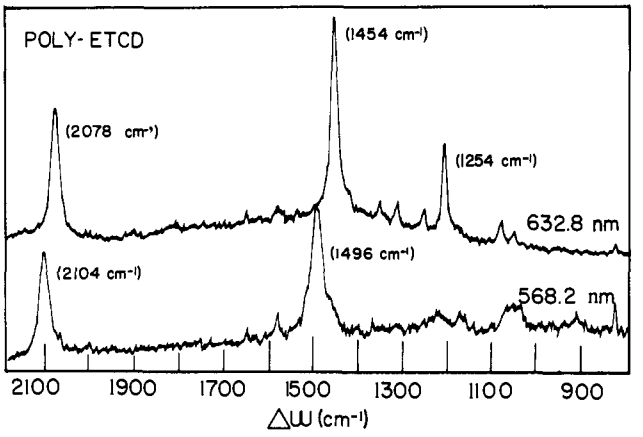


Figure 2. Room-temperature Raman spectra of poly-ETCD with 632.8- and 568.2-nm excitation.

Raman effect (RRE). Thus, with the 632.8 nm (or 647.1 nm) source $\nu$(C=C) and $\nu$(C≡C) proper to domain 1, which absorbs light at 630 nm, are observed as resonance-enhanced bands. They are much more intense than those at the $\nu$(C=C) and $\nu$(C≡C) values for domains 2 or 3. When 530.8 nm (or 568.2 or 514.5 nm) radiation is used, bands at the $\nu$(C=C) and $\nu$(C≡C) proper to domain 2, which absorbs light at 540 nm, are resonantly enhanced and dominate the Raman spectrum. Finally, with 488.0 nm (or 457.9 nm) radiation, bands at the values of $\nu$(C=C) and $\nu$(C≡C) for domain 3, which absorbs at 460 nm, are observed.

This interpretation presumes that the distribution in delocalization lengths peaks about the three values $l_1$, $l_2$, and $l_3$, except for very short lengths which would give rise to ultraviolet absorption. Thus, the position of $\nu$(C=C) or $\nu$(C≡C) in a given spectrum reflects its value in the domain whose electronic transition is in resonance with the source. This is borne out by the fact that the spectrum taken with 514.5-nm radiation contains peaks for two of the domains, as shown clearly in Figure 3 for $\nu$(C=C).

**Variable-Temperature Raman Spectra.** The Raman spectrum of a 100-Mrad poly-ETCD sample changes as its temperature is raised. Again, the nature of the change depends upon the source frequency. With a 632.8-nm source the vibrational band observed at room temperature, either $\nu$(C=C) or $\nu$(C≡C), remains at the same frequency as the temperature is raised to 100°C. However, as shown in Figures 4 and 5, when the temperature reaches 120°C this band decreases in intensity and a higher frequency band appears. At 136°C, just above the green to red-phase transition, the $\nu$(C=C) and $\nu$(C≡C) bands occur with a red-light source at the same frequencies at which they are observed at room temperature with the yellow (568.2 nm) source. Thus, $\nu$(C=C) is 1454 cm$^{-1}$ at 25°C and 1496 cm$^{-1}$ at 136°C with the 632.8-nm source.

This result can be interpreted on the same basis as the room-temperature Raman spectra. Thus, as the material passes through the thermochromic phase transition the fraction of domains having delocalization lengths $l_1$ decreases, and that of lengths $l_2$ increases. Despite the resonance enhancement of vibrational bands for domain 1 by red light, the Raman bands proper to domain 2 are ob-

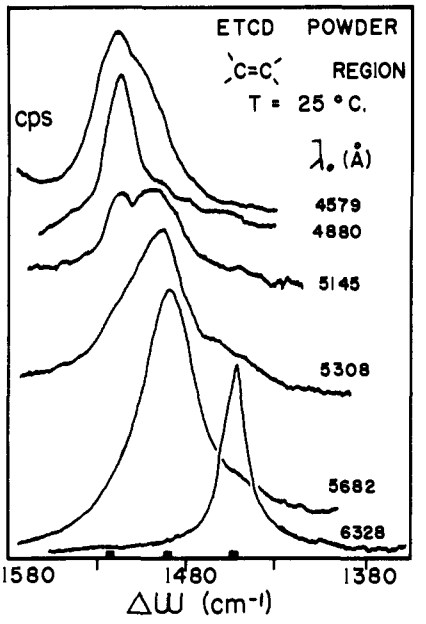


Figure 3. Room-temperature Raman spectra of poly-ETCD, obtained with low-power excitation at the wavelengths $\lambda_0$ in the $\nu$(C=C) region.

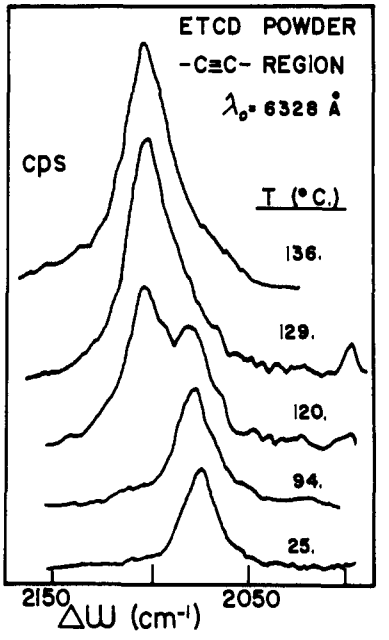


Figure 4. Temperature-dependent Raman spectra of poly-ETCD under 632.8-nm excitation (1-mW incident power) in the $\nu$(C≡C) region.

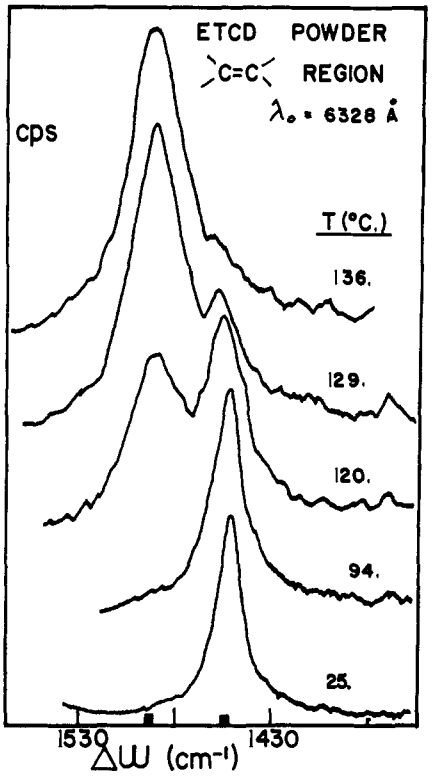


Figure 5. Temperature-dependent Raman spectra of poly-ETCD under 632.8-nm excitation (<1 mW incident laser power) in the $\nu$(C=C) region.

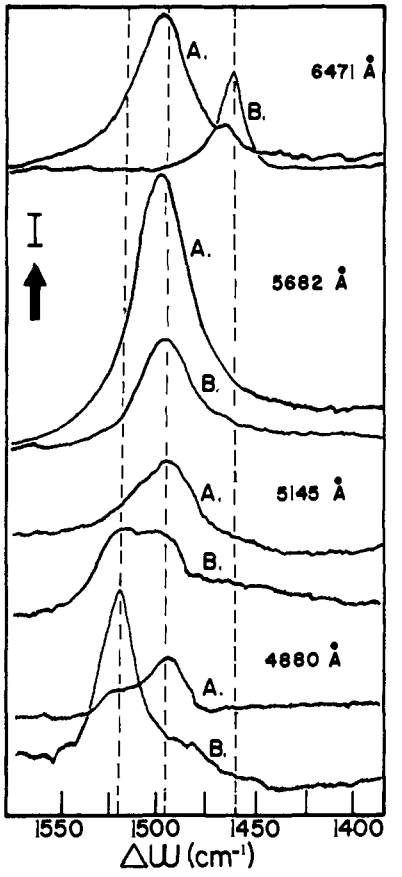


Figure 6. Raman spectra of poly-ETCD in the $\nu$(C=C) frequency region excited by several laser lines. Spectra labeled B were obtained with the sample at 25°C and spectra labeled A were obtained with it just above the thermochromic transition (136°C).

served simply because there are very few domain 1 regions present.

When the same experiments are done using the blue (488.0 nm) Raman source, the $\nu$(C≡C) and $\nu$(C=C) vibrational bands observed at room temperature are replaced, as the temperature is raised to 136°C, by bands at the frequencies observed at room temperature with yellow (568.2 nm) light. Thus, $\nu$(C=C) is 1525 $cm^{-1}$ at 25°C and 1496 $cm^{-1}$ at 136°C with the 488.0-nm source. This result also indicates that the distribution of coherence lengths peaks around $l_2$ as the temperature of poly-ETCD is raised through the phase transition.

This interpretation requires that the band, either $\nu$(C=C) or $\nu$(C≡C), observed at room temperature with yellow light (568.2 nm) remains at the same frequency and becomes more intense as the temperature of the poly-ETCD is raised to 136°C. Indeed, this is the case, as shown in Figure 6. In that figure it is shown that the $\nu$(C=C) value of 1496 $cm^{-1}$ dominates above the thermochromic phase transition, regardless of the Raman source's frequency. The low-temperature spectral results are again obtained upon sample cooling, and upon cycling the same temperature identical spectral results are obtained reversibly.

This is taken to mean that the effect of the phase transition is to peak the distribution of delocalization lengths at a value near $l_2$.

**Thermal Analysis.** The results of DSC experiments showed that the 25-, 50-, and 100-Mrad samples of poly-ETCD have an essentially reversible phase transition at about 135°C. In runs in which the sample was successively heated and cooled the transition temperature, $T_t$, decreased about one degree centigrade per cycle for the first few cycles, with the broad transition always in the 117-137°C range. In DTA scans a reproducible endotherm was found at 135°C, the temperature of the color change. However, the 1- and 5-Mrad dosed samples, which do not change color, do not have an endotherm, and they give no evidence by DSC of having any transition below 150°C. There is, at most, negligible (<0.5%) weight-loss decomposition on heating the samples to 200°C, as shown by TGA measurements. However, nearly complete decomposition occurs above 250°C. There is no measurable weight loss at $T_t$ for any of the samples.

Since the thermal studies show that a nearly reversible, endothermic phase transition accompanies the color change in poly-ETCD samples at 135°C, making and breaking of covalent bonds is not involved in the phase change.

## Free Electron Gas Model

The results presented above show that dramatic changes in the Raman spectra of poly-ETCD occur as the source frequency is varied and as the material is heated through its thermochromic phase transition at 135°C. The general interpretation was based on the assumption that there exist sections of polymer molecules over which $\pi$ electrons are delocalized. In such a section, or domain, of delocalization length $l$, the electron density is uninterrupted, but a discontinuity occurs at each end of the domain. A domain may be only a few monomer units long, and, in general, there can be many different domains of different lengths on any one polymer molecule. The domains can be terminated either by an end of the polymer molecule or by a configurational distortion which causes the $\pi$-type overlap of orbitals on adjacent carbon atoms to be negligible.

Three known phenomena support the interpretation qualitatively. First, Ivanova and coworkers have shown that, in a series of molecules of the form R-(CH=CH)$_n$-R, the value of $\nu$(C=C) decreases monotonically from 1664 to

Table I. The Position $\lambda_{max}^{-1}$ of the Longest Wavelength Absorption Peak for All-Trans Polyenes and Polyenynes Containing $2n$ Conjugated Multiple Bonds

| $2n$ | Compd | $\lambda_{max}^{-1}$, $cm^{-1}$ | Ref |
|---|---|---|---|
| 2 | $H(HC{=}CH)_2H$ | 45 980[a] | 18 |
| | $H_3C(HC{=}CH)_2CH_3$ | 44 200[a] | 16 |
| | $H_2C{=}CH{-}C{\equiv}CH$ | 43 950[c] | 19 |
| | $H_3CCH{=}CH{-}C{\equiv}C{-}CH_3$ | 44 900[b] | 20 |
| 3 | $H(HC{=}CH)_3H$ | 37 300[c] | 21 |
| | $H_3C(HC{=}CH)_3CH_3$ | 36 430[f] | 16 |
| | $H_2C{=}CH{-}C{\equiv}C{-}CH{=}CH_2$ | 37 600[c] | 19 |
| | $H(HC{=}CH)_2C{\equiv}CH$ | 37 700[c] | 19 |
| | $HC{\equiv}C{-}CH{=}CH{-}C{\equiv}CH$ | 38 200[d] | 22 |
| | $H_3C{-}C{\equiv}C{-}HC{=}CH{-}C{\equiv}C{-}CH_3$ | 36 900[c] | 17 |
| | $H_3CCH{=}CH{-}C{\equiv}C{-}CH{=}CHCH_3$ | 36 400[b] | 20 |
| 4 | $H(HC{=}CH)_4H$ | 32 900[e] | 21 |
| | $H_3C(HC{=}CH)_4CH_3$ | 32 300[f] | 16 |
| | $H(HC{=}CH)_3C{\equiv}CH$ | 33 500[c] | 19 |
| | $H(HC{=}CH)_2C{\equiv}C{-}CH{=}CH_2$ | 33 400[c] | 19 |
| | $H_3C(HC{=}CH)_2{-}C{\equiv}C{-}CH{=}CH{-}CH_2OH$ | 32 700[b] | 23 |
| | $HC{\equiv}C(HC{=}CH)_2C{\equiv}CH$ | 33 900[a] | 24 |
| 5 | $H(HC{=}CH)_5H$ | 29 940[c] | 21 |
| | $H_3C(HC{=}CH)_5CH_3$ | 29 300[f] | 16 |
| | $H_3C(HC{=}CH)_2{-}C{\equiv}C{-}(HC{=}CH)_2CH_2CH_3$ | 29 700[b] | 25 |
| 6 | $H(HC{=}CH)_6H$ | 27 500[c] | 21 |
| | $H_3C{-}C{\equiv}C{-}(HC{=}CH)_4{-}C{\equiv}C{-}CH_3$ | 27 600[f] | 26 |
| 7 | $H(HC{=}CH)_7H$ | 25 600[c] | 21 |
| | $H(HC{=}CH)_6{-}C{\equiv}CH$[g] | 26 000[c] | 17 |
| 8 | $H(HC{=}CH)_8H$ | 24 400[c] | 21 |
| | $H_3C(HC{=}CH)_8CH_3$ | 23 800[b] | 16 |
| 9 | $H_3C(HC{=}CH)_9CH_3$ | 22 700[b] | 16 |
| | $H_3C(HC{=}CH)_4{-}C{\equiv}C{-}(HC{=}CH)_4CH_3$ | 23 560[b] | 16 |
| 10 | $H(HC{=}CH)_{10}H$ | 22 400[c] | 21 |

[a] Ethanol solution. [b] Ether or petroleum ether solution. [c] Isooctane solution. [d] Methanol solution. [e] Cyclohexane solution. [f] *n*-Hexane solution. [g] Conformation not reported.

1540 $cm^{-1}$ as $n$ is varied from 1 to 8. Clearly, $\nu$(C=C) depends on what we have called the coherence length; it decreases as $l$ increases.[8]

Second, the resonance Raman effect permits a vibrational band to be selectively intensified when the source frequency comes into resonance with an electronic transition of the system containing the oscillator. Thus, the frequency of a source which causes the vibration for a given domain to be most intense is in or near resonance with the electronic transition of that domain.

Third, the electronic transition frequency of an electron in a one-dimensional box is decreased as the length of the box is increased. Thus, the lowest frequency absorption feature is associated with the domains of greatest length and lowest values of $\nu$(C=C) and $\nu$(C≡C).

In the domains under consideration there are more electrons than one, and these $\pi$ electrons may be considered as a one-dimensional electron gas. By confining it to a certain length, $l$, over which it is subject to a potential which is constant over $l$ but infinite at the bounds of $l$, the Schrödinger equation may be solved for the allowed electronic energy levels. For one electron:

$$E = h^2m^2/8Ml^2 \qquad (1)$$

and

$$\Delta E = E_{m+1} - E_m = (2m + 1)h^2/8Ml^2 \qquad (2)$$

where the quantum number $m$ takes positive integer values 0, 1, 2, 3, . . ., $h$ is Planck's constant, $M$ is the electron's mass, and $l$ is the coherence length. This model was applied to polymethine dye molecules by Kuhn[9,10] to explain their visible absorption spectra.

In order to make the calculation more realistic Kuhn also assumed a periodically varying potential within the domains.[10] This introduces a perturbation on the energy levels given by eq 1 above, and the solution to the Schrödinger equation becomes a function of the barrier height, $V_0$, of the sinusoidal potential, and the number of $\pi$ electrons ($N$) in the system:

$$\Delta E = \frac{h^2}{8Ml^2}(N + 1) + 0.83V_0\left(1 - \frac{1}{N}\right) \qquad (3)$$

This equation could be used to predict the visible spectrum of poly-ETCD *approximately*, if $V_0$ and $l$ were known. ($N$ is determined for a given $l$.) However, since a distribution in delocalization lengths is predicted in our interpretation of the spectral results, it is preferable to estimate $V_0$ and calculate an average value for $l$ for each band observed in the visible absorption spectrum.

To estimate $V_0$, we note Kuhn's results for polyenes and polyacetylenes of various chain lengths. He found[10] that good agreement is obtained between the band gap calculated via eq 3 and the long-wavelength optical transition for each member of the series of polyenes and polyacetylenes, of varying chain length, if $V_0$ is taken as 2.4 eV (19 400 $cm^{-1}$) for polyenes and 3.4 eV (27 400 $cm^{-1}$) for polyacetylenes.

The polydiacetylenes, of interest here, have in common with the polyenes the similarity that for both the polydiacetylene "backbone" segment [=C—C≡C—C=] and the polyene segment [=C—C=C—C=] there are four electrons in orbitals which are capable of substantial $\pi$ overlap. The remaining two electrons in $\pi$ orbitals in the polydiacetylene are in orbitals which are orthogonal to the

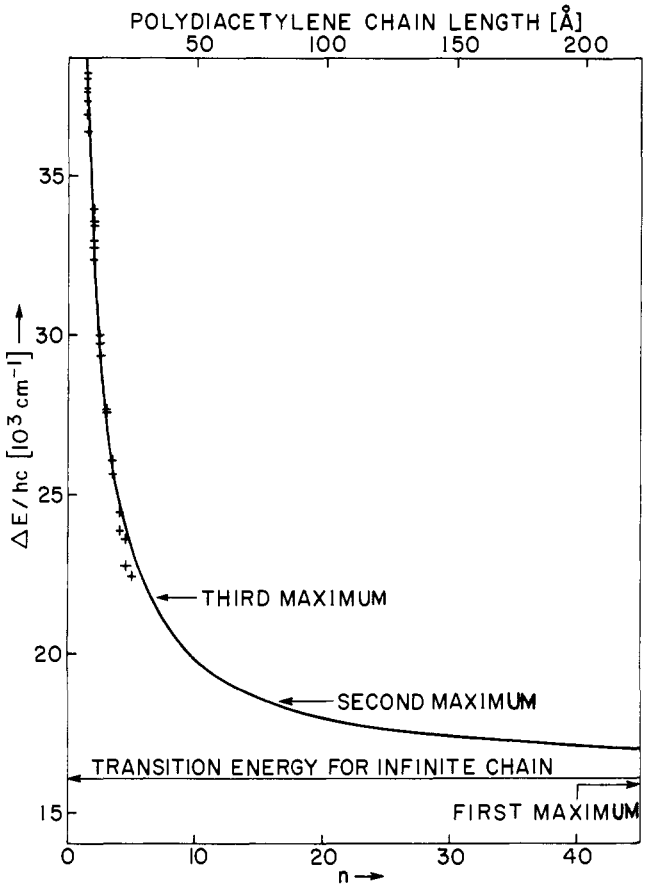


Figure 7. Calculated $\pi$-$\pi^*$ transition energy as a function of $n$, the number of monomer units ($C_4R_2$) in the chain. The observed absorption energies for polyenes and polyenynes (Table I) containing the same number of multiple bonds are indicated by the data points. The arrows indicate the observed absorption energies for poly-ETCD.

ones containing the four electrons mentioned above. Due to the similarity of polydiacetylene and polyene bond structure, to treat the four electrons of the polydiacetylenes in the present modified free-electron approximation it is reasonable to take the bond potential difference between the centers of all multiple bonds and the adjacent single bonds to be identical and equal to the above value of $V_0$ for the polyenes. This is done in order for the sinusoidal potential superimposed on the square well potential to be self-consistent with the electron distribution, which is known to consist approximately of two of these $\pi$ electrons at the triple bond and the remaining two at the double bond.

The reliability of this approach may be seen by considering the values of $\lambda_{max}^{-1}(cm^{-1})$ for the longest wavelength absorption peak in polyenes and polyenynes listed in Table I. As shown there and observed earlier,[16,17] replacing one or more nonsuccessive double bonds in the polyenes with triple bonds results only in a small change in this transition energy, so it is reasonable to take the same value of $V_0$ to be used both for polyenes and for polyenynes such as the polydiacetylenes.

A polydiacetylene chain with $n$ conjugated monomer repeat units contains $N$ ($N = 4n$) electrons in overlapping $\pi$ orbitals and has an effective length, $l$,

$$l = n\{d(C{\equiv}C) + d(C{=}C) + 2d(C\text{-}C)\} + d(C\text{-}C) \quad (4)$$

where $d(C{\equiv}C)$, $d(C{=}C)$, and $d(C\text{-}C)$ are carbon-carbon bond lengths. This total length includes a contribution (one-half) from a carbon-carbon single bond at each end of the chain, so that $\pi$-electron density is not abruptly terminated by an infinite potential wall at the multiply bonded carbon atoms at the chain ends. Employing reported values[11] for carbon-carbon bond lengths in the polydiacetylenes,

$$l(\text{nm}) = 0.539n + 0.141 \quad (5)$$

Expressing eq 3 for the polydiacetylenes, the lowest energy transition is found to be

$$\Delta E = \frac{h^2}{8Ml^2}(4n + 1) + 0.83V_0\left(1 - \frac{1}{4n}\right) \quad (6)$$

This is the expression obtained for a polyene chain containing the same number of multiple bonds, if small differences in corresponding values of $l$ are neglected.

The transition energies calculated using eq 6 are plotted in Figure 7, which also contains points representing the observed long-wavelength optical absorption peak for each of the polyenes and polyenynes listed in Table I. Employing this relationship and the observed absorption peak frequencies of poly-ETCD as marked on Figure 7, it is calculated that the longest domains in poly-ETCD have an effectively infinite (>20 nm) delocalization length, the intermediate length domains contain approximately 16 monomer units, corresponding to a delocalization length of about 8.0 nm, and the shortest length domains contain approximately 6 monomer units, corresponding to a domain length of about 3.0 nm.

## Discussion

Changes in the Raman observed $\nu_{C=C}$ and $\nu_{C\equiv C}$ frequencies, which occur as the Raman source frequency is changed, suggest the existence in poly-ETCD of a distribution of "domains" over which $\pi$ electrons are delocalized. Furthermore, the distribution of the domains appears to have at least three maxima, since three different Raman bands can be observed in the $\nu_{C=C}$ or $\nu_{C\equiv C}$ regions, with the bands observed in a given spectrum being dependent on the source frequency. Further evidence which is consistent with the existence of three different regions of $\pi$-electron delocalization is seen in the room-temperature visible absorption spectrum of poly-ETCD, in which three broad bands are resolved and assigned to $\pi$-electron transitions for each of these regions. Thus, the room-temperature Raman spectra are consistent with three $\pi$-electron delocalization lengths predominating in the distribution of such lengths in the polymer, and, through a resonance Raman effect, Raman spectra characteristic of one domain may be greatly enhanced over Raman spectra characteristic of the other domains.

The room-temperature Raman results and their interpretation are useful in discussing changes on a molecular scale which accompany the thermochromic phase transition of poly-ETCD.

The near reversibility of the phase transition seen in both Raman and DSC experiments suggests that no bond breaking in the polymer occurs. In addition, thermochromism in poly-ETCD is certainly influenced by the nature of the R group and related lattice packing in the polymer, since this phase transition is not observed for all polydiacetylenes; e.g., no thermochromism below the melting or degradation temperature is observed for the analogous polydiacetylenes with substituent groups $(CH_2)_nOCONHC_2H_5$, where $n$ = 2 or 3.

The room-temperature Raman results show that basically three $\pi$-electron delocalization domains are present. Above $T_t$ essentially only one $\nu_{C=C}$ vibration is observed regardless of the frequency of the incident laser light and this implies that one $\pi$-electron delocalization domain dominates above $T_t$. The model, then, is of a polymer which has three dominant delocalization lengths at room temperature and one above $T_t$. It is plausible that at the lower tempera-

ture there are three slightly different chain types which differ in chain conformation and, therefore, in extent of $\pi$-electron delocalization. These differences could result in part from differences in lattice packing and intermolecular interactions, the latter via hydrogen or van der Waals bonding, and would constrain the chain to three slightly different environments. This model suggests, then, that at high temperatures an increase in mean-square vibrational amplitudes occurs which causes a decrease in the weakly attractive R group interactions, allows all chains to be equivalent, and results in a new distribution of $\pi$-electron delocalization lengths. At lower temperatures the weak interactions are reestablished as is the low-temperature distribution in $\pi$-electron delocalization lengths.

In quantum mechanical terms, the "free-electron molecular-orbital model", FEMO, we have used is a "naive" treatment of $\pi$-electron systems because its wave functions are not strictly eigenfunctions of the actual total-molecular hamiltonian, but it has several advantages. One is obviously the simple functional dependence of the energy on $L$. Another[12,13] is that the FEMO wave functions accurately correspond to the Huckel molecular orbital (HMO) orbital coefficients and the energy level spacings agree at an HMO resonance parameter of $\beta = -\hbar^2/2mD^2$, where $D$ is the chain repeat dimension as measured along the bond lengths.

Employing a band theory approach, which assumes separability of $\sigma$ and $\pi$ states and applies Huckel theory, Wilson[14] has calculated that the band gap for an infinite conjugation length polydiacetylene is given by $\Delta E = |\gamma_3|$ where $\gamma_3$ is a combination of resonance parameters, $\beta$. As Wilson has pointed out, the thus calculated band gap of 1.36 eV is only approximate because it is the difference of poorly established values of $\beta$. In the present case $\Delta E$ for the longest delocalization length is approximately 1.9 eV, as compared to the present predicted value of 2.0 eV for an infinite chain. In a recent study of the optical reflectance spectra of the polydiacetylene with R = $p$-toluenesulfonate, Bloor et al.[15] found that the main peak splits into two peaks as the temperature is lowered. Although several possible interpretations were presented by the authors,[15] the suggestion is made that two slightly different chains may exist in the lower temperature regime and that one exists at higher temperature. This is consistent with our interpretation of the temperature-dependent Raman data on poly-ETCD.

**Acknowledgment.** This work was supported in part by the Office of Naval Research. The authors are grateful to E. A. Turi for the TGA, DTA, and DSC measurements and analysis and to A. F. Preziosi for polymer synthesis, and to the late Vijay K. Mitra for helpful discussions. The partial support and use of the facilities of the Materials Science Program at Brown University, supported by the National Science Foundation, is gratefully acknowledged.

## References and Notes

(1) (a) Brown University; (b) Allied Chemical Corporation.
(2) (a) A. J. Melveger and R. H. Baughman, *J. Polym. Sci., Polym. Phys. Ed.*, **11** 603 (1973); (b) R. H. Baughman, G. J. Exarhos, and W. M. Risen, Jr., *J. Polym. Sci., Polym. Phys. Ed.*, **12**, 2189 (1974).
(3) R. H. Baughman, J. D. Witt, and K. C. Yee, *J. Chem. Phys.*, **60**, 4755 (1974).
(4) R. H. Baughman, *J. Appl. Phys.*, **43(11)**, 4362 (1972).
(5) G. Wegner, *Z. Naturforsch., B*, **24**, 824 (1969).
(6) G. Wegner, *Polym. Lett.*, **9**, 133 (1971).
(7) G. Wegner, *Makromol. Chem.*, **145**, 85 (1971).
(8) T. M. Ivanova, L. A. Yanovskaya, and P. P. Shorygin, *Opt. Spectrosc. (USSR)*, **18**, 206 (1965).
(9) H. Kuhn, *J. Chem. Phys.*, **17(12)**, 1198 (1949).
(10) H. Kuhn, *Fortschr. Chem. Org. Naturst.*, **17**, 404 (1959).
(11) E. Hädicke, E. C. Mez, C. H. Krauch, G. Wegner, and J. Kaiser, *Angew. Chem.*, **83**, 253 (1971).
(12) H. H. Jaffé, *J. Chem. Phys.*, **21**, 1287 (1953).
(13) J. R. Platt et al., "Free-electron Theory of Conjugated Molecules: A Source Book", Wiley, New York, N.Y., 1965.
(14) E. G. Wilson, private communication.
(15) D. Bloor, D. J. Ando, F. H. Preston, and G. C. Stevens, *Chem. Phys. Lett.*, **24**, 407 (1974).
(16) Von U. Schwieter, H. R. Bollinger, L. H. Schopard-Dit-Gean, G. Englert, M. Kofler, A. König, C. V. Planta, R. Rüegg, W. Vetter, and O. Isler, *Chimia*, **19**, 294 (1965).
(17) Y. Gaoni, C. C. Leznoff, and F. Sondheimer, *J. Am. Chem. Soc.* **90**, 4940 (1968).
(18) W. F. Forbes and R. Shilton, *J. Org. Chem.*, **24**, 436 (1959).
(19) K. K. Greorgieff, W. T. Cave, and K. G. Blaikie, *J. Am. Chem. Soc.*, **76**, 5494 (1954).
(20) "Uv Atlas of Organic Compounds", Vol. III, Plenum Press, New York, N.Y., 1967.
(21) F. Sondheimer, D. A. Ben-Efraim, and R. Wolovsky, *J. Am. Chem. Soc.*, **83**, 1675 (1961).
(22) T. Böhm-Gössl, W. Hunsmann, L. Rohrschneider, W. M. Schneider, and W. Ziegenbein, *Chem. Ber.*, **96**, 2504 (1963).
(23) F. Bohlmann, K. M. Kleine, and H. Bornowski, *Chem. Ber.*, **98**, 369 (1965).
(24) G. H. Mitchell and F. Sondheimer, *J. Am. Chem. Soc.*, **91**, 7520 (1969).
(25) F. Bohlmann, L. Fanghänel, M. Wotschokowsky, and J. Laser, *Chem. Ber.*, **101**, 2510 (1968).
(26) H. Straub, J. M. Rao, and E. Müller, *Justus Liebigs Ann. Chem.*, 1339 (1973).